JMEPEG (2011) 20:969–977
DOI: 10.1007/s11665-010-9719-9

1059-9495/$19.00

Studies on a Few Substituted Piperidin-4-one Oximes as Corrosion Inhibitor for Mild Steel in HCl

A.N. Senthilkumar, K. Tharini, and M.G. Sethuraman

(Submitted November 20, 2009; in revised form May 26, 2010)

The corrosion inhibition of mild steel in 1 M hydrochloric acid by a few piperidin-4-one oxime derivatives, namely, 1,3-dimethyl-2,6-diphenyl piperidin-4-one oxime (I), 3,3-dimethyl-2,6-diphenyl piperidin-4-one oxime (II), and 3-isopropyl-2,6-diphenyl piperidin-4-one oxime (III) was studied using chemical weight loss method, electrochemical polarization and impedance spectroscopy, SEM with EDS, XRD, FT-IR measurements, and semi-empirical AM1 method for electronic properties. The weight loss measurements at four different temperatures such as 30, 40, 50, and 60 °C showed that the percentage inhibition efficiency (IE) of these compounds increased with increase of concentration and decreased with increase of temperature. The IE followed the order III < II < I. It was found that these inhibitors function through physical adsorption mechanism obeying Temkin's isotherm. Polarization studies showed that these compounds act as mixed-type inhibitors. Impedance measurements revealed the increase of charge transfer resistance with inhibitor concentration. Surface analysis using SEM, XRD, and FT-IR revealed the formation of protective film over the mild steel surface. The electronic properties calculated using AM1 semi-empirical method explained the inhibition characteristics. The quantum chemical studies showed that ring nitrogen and phenyl rings are the probable active centers to inhibit corrosion process.

Keywords impedance, mild steel, polarization, SEM, XRD

1. Introduction

Dissolution of mild steel has been extensively studied in acidic media, and the mechanism of the process has been the subject of both practical and theoretical importance. Organic compounds containing polar atoms like oxygen, nitrogen, phosphorus, or sulfur have been widely studied as inhibitors for the acid corrosion of steel (Ref 1, 2). Their inhibitive effect is due to the adsorption of inhibitor molecules onto the metal surface following known adsorption isotherms (Ref 3). Adsorption affects the cathodic and anodic reactions to varying extents. The electrostatic attraction between the charged hydrophilic groups and the charge centers on the metal surface leads to physisorption. Availability of lone pair and π electrons in alkenes, alkynes, and aromatic rings in the inhibitor molecules may contribute for chemisorption. The strength of the coordinate bond formed depends on the electron density and polarizability of the donor atom of the functional group (Ref 4). The existing data show that the organic inhibitors adsorb on the metal surface by displacing water molecules on the surface and form a compact barrier film (Ref 5).

Piperidin-4-one oximes, an important class of organic compounds, are extensively studied as molecules of biological interest (Ref 6). In this study, we have synthesized a few piperidin-4-one oximes with varying degree of steric crowding around the oxime nitrogen and their effects on the corrosion inhibition of mild steel in 1 M hydrochloric acid solutions have been investigated.

A.N. Senthilkumar and **K. Tharini**, Department of Chemistry, SASTRA University, Thanjavur 613 402, India; and **M.G. Sethuraman**, Department of Chemistry, Gandhigram Rural University, Gandhigram 624 302, India. Contact e-mail: mgsethu@rediffmail.com.

2. Experimental

2.1 Preparation of Piperidin-4-one Oximes

1,3-Dimethyl-2,6-diphenyl-piperidin-4-one, 3,3-dimethyl-2,6-diphenyl-piperidin-4-one, and 3-isopropyl-2,6-diphenyl-piperidin-4-one were prepared by the method of Baliah and Noller (Ref 7). A mixture of 8.3 mL of aqueous 40% methyl amine solution or ammonium acetate, 21.2 mL (1.5 mol) of benzaldehyde, and 10 mL of (1 mol) substituted ketone in 20 mL of glacial acetic acid was heated to boiling and allowed to stand overnight. Addition of concentrated hydrochloric acid to the above mixture gave the hydrochloride. Then, the free base was obtained by the neutralization of the hydrochloride suspended in acetone with aqueous ammonia followed by distillation, and it was recrystallized from ethanol.

Then, these ketones were treated with filtrate formed from mixing of hydroxyl amine hydrochloride and sodium acetate in ethanol and refluxed for 4 h and finally poured into water. The products, viz., **I**, **II**, and **III** were recrystallized from ethanol and duly characterized using ^{1}H and ^{13}C NMR spectra whose structures are depicted in Fig. 1.

2.2 Weight Loss Method

The mild steel specimens with chemical composition (wt.%) C = 0.15, Mn = 0.36, S = 0.28, P = 0.09, Si = 0.017, and the rest Fe were used as working specimens of length: 4 cm, width: 1 cm, and thickness: 0.2 cm. They were polished with emery

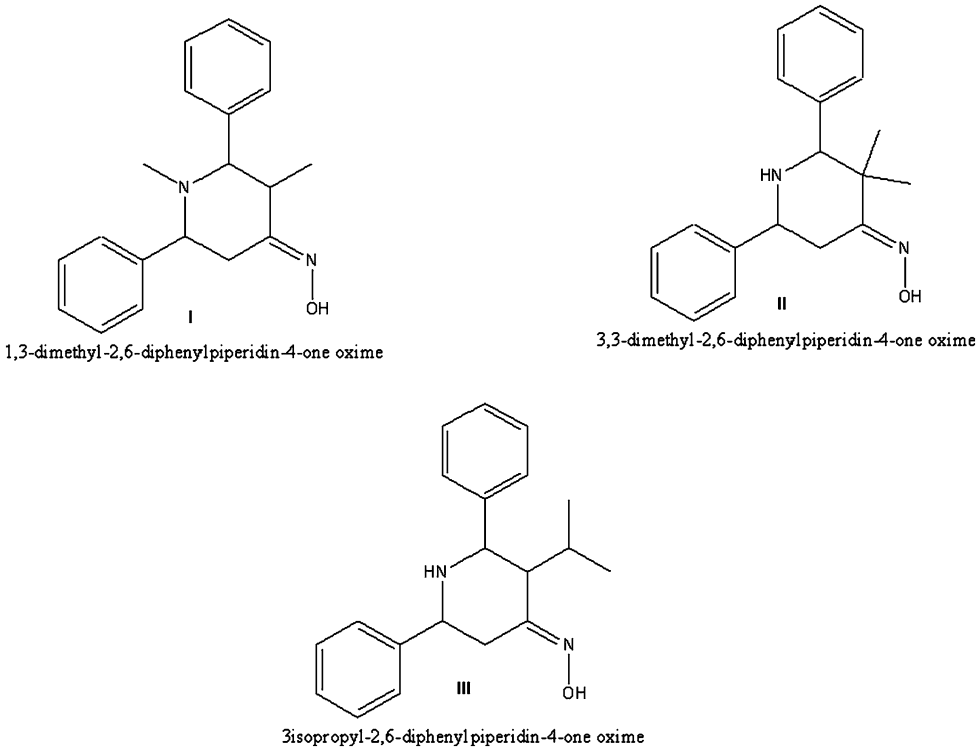

Fig. 1 Structures of the studied compounds

papers of various grades, cleaned with acetone, washed with double-distilled water, and finally dried at room temperature before being immersed in the acid solution with and without inhibitor. Using the hydrochloric acid solution (1 M), various concentrations of inhibitor viz., 25, 50,100, 150, 200, 250, 300, 400, and 500 ppm were prepared. Loss in weights was determined at four different temperatures (30, 40, 50, and 60 °C) for 1- and 2-h-time durations. At the end of the tests, the specimens were carefully washed in water, dried, and then weighed.

2.3 Electrochemical Studies

Electrochemical experiments were carried out using CHI 604C potentiostat. A three-electrode electrochemical cell was used. The working electrode was prepared from a mild steel sheet, such that the area exposed to solution was 1 cm^2. A saturated calomel electrode (SCE) and a platinum electrode were used as the reference and the counter electrode, respectively. The potentiodynamic polarization measurements made from −0.15 to −0.75 V of 1 mV/s. The open circuit potential (OCP) values were recorded after 1-h immersion at 30 °C for working electrode in test solution with and without various concentrations of the studied inhibitors. EIS measurements were carried out at steady state OCP perturbed with amplitude of 10 mV a.c. sine wave. The monitored frequency range was between 100 kHz and 10 mHz. The simple equivalent circuit diagram for stimulated metal/solution interface is presented in Fig. 2 wherein C_{dl} refers to the double layer capacitance, R_s is the solution resistance, and R_{ct} denotes the charge transfer resistance.

2.4 SEM with EDS

The mild steel specimens of dimension 1 × 1 × 0.1 cm with a small hole having composition as specified earlier were used for the entire SEM study. They were abraded with emery papers, degreased with acetone, dried and preserved in a desiccator prior to the use. Surface morphological characteristics of the inhibited and uninhibited samples were recorded after 2-h immersion in acid medium using SEM (Philips XL series) instrument coupled with energy dispersive spectrometer (EDS). The optimum concentration for recording SEM was fixed as 500 ppm of the studied oximes at 303 K for 2-h duration, because the oximes show their maximum efficiency under these conditions.

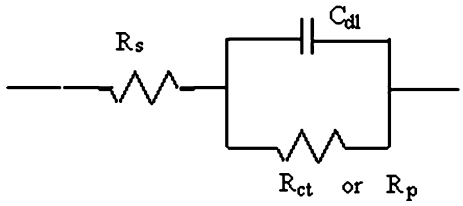

Fig. 2 Equivalent circuit diagram for stimulated metal/solution interface

2.5 XRD Measurements

Diffraction pattern of brightly polished mild steel surface and film formed by inhibitor over the surface of mild steel were examined after 24-h immersion using inel XRD instrument employing Cu Kα radiation (wavelength 1.54 Å) and a diffracted beam monochromator. Patterns were collected at a scan rate of 1°/min. The specimen preparation, inhibitor concentration, and temperature used for measuring patterns were similar to those for SEM studies. The specimens were subsequently washed with distilled water, dried, and desiccated for recording the XRD pattern.

2.6 Quantum Chemical Study

Quantum chemical parameters for inhibitors, obtained using the AM1 semi empirical quantum chemical approach in Chemoffice 2004 package, were correlated with their experimentally determined inhibition efficiencies. The quantum chemical indices such as the energy of the highest occupied molecular orbital (E_{HOMO}), the energy of the lowest unoccupied molecular orbital (E_{LUMO}), and probable electron donating sites to control the corrosion process were computed and analyzed.

2.7 IR Studies

The IR spectra of the compound **I**, as well as the adsorbed film of this compound over mild steel surface, were recorded using the Perkin Elmer-1600 spectrophotometer.

3. Results and Discussion

3.1 ^{1}H and ^{13}C NMR Data

The ^{1}H and ^{13}C NMR data of the synthesized compounds are given here, and the characterization was done using the spectral data.

Compound **I** ^{1}H NMR ($CDCl_3$): 0.9 (s, 3H, NCH_3), 2.1 (d, 1H, C2), 1.3 (m, 1H, C3) 1.2 (m, 2H, C5), 1.6 (t, 1H, C6), 0.8 (d, 3H, CH_3), 3.1 (s, 1H, -N-OH), 7.3 (m, 10H, Ar-H).

Compound **I** ^{13}C NMR ($CDCl_3$): 67.1 (C2), 41.9 (C3), 158.2 (C4), 34.3 (C5), 72.6 (C6), 29.0 (N-CH_3), 18.7 (CH_3), 125.3-129.5 (Aromatic carbons).

Compound **II** ^{1}H NMR ($CDCl_3$): 1.9 (s, 1H, -NH), 2.2 (s, 1H, C2), 1.3 (d, 2H, C5), 1.85 (m, 1H, C6), 3.2 (s, 1H, -N-OH), 0.80 (s, 3H, CH_3), 0.85 (s, 3H, CH_3), 7.4 (m, 10H, Ar-H).

Compound **II** ^{13}C NMR ($CDCl_3$): 67.1 (C2), 42.3 (C3), 158.2 (C4), 27.7 (C5), 72.6 (C6), 17.7 (CH_3), 125.0-129.1 (Aromatic carbons).

Compound **III** ^{1}H NMR ($CDCl_3$): 1.8 (s, 1H, -NH), 2.3 (m, 1H, C2), 2.4 (m, 1H, C6), 2.2 (m, 1H, C3), 1.0 (m, 2H, C5), 3.0 (s, 1H, -N-OH), 2.0 (m, 1H, CH), 0.8 (dd, 6H, CH_3), 7.35(m, 10H, Ar-H).

Compound **III** ^{13}C NMR ($CDCl_3$): 67.1 (C2), 38.2 (C3), 160.1 (C4), 21.3 (C5), 69.2 (C6), 29.0 (CH) 12.3 (CH_3) 125.0-129.1 (Aromatic carbons).

3.2 Weight Loss Studies

The results obtained from weight loss measurements for different concentrations of **I**, **II**, and **III** at 30-60 °C are given in Table 1. The values of IE were calculated using Eq 1.

$$IE = 100 \times \left(1 - \frac{W_p}{W_a}\right) \quad \text{(Eq 1)}$$

where W_p is the weight loss in the presence of inhibitor and W_a is the weight loss in absence of inhibitor.

Table 1 Inhibition efficiencies obtained from the weight loss measurements for mild steel in different concentrations of piperidin-4-one oximes in 1 M HCl

		IE							
		30 °C		40 °C		50 °C		60 °C	
Compound	Concentration, ppm	1 h	2 h	1 h	2 h	1 h	2 h	1 h	2 h
I	25	62.9	65.8	60.4	61.3	59.2	60.0	55.0	58.3
	50	66.1	68.3	63.2	64.6	60.4	61.6	57.6	60.0
	100	68.9	70.7	65.4	67.8	62.2	65.3	61.3	62.2
	150	70.3	74.0	68.9	71.6	65.3	66.6	62.2	63.3
	200	75.3	77.7	73.2	75.4	66.8	69.8	64.8	66.5
	250	78.1	79.4	76.9	77.8	70.0	74.5	68.3	70.6
	300	83.4	84.7	79.0	79.4	72.7	76.9	69.4	71.3
	400	86.2	87.2	80.1	80.9	74.2	78.2	70.2	72.2
	500	89.4	93.4	80.9	84.0	78.3	79.7	73.1	74.5
II	25	63.3	65.8	60.4	61.3	58.4	59.4	50.2	54.2
	50	65.0	67.1	63.2	64.6	60.2	61.3	51.3	55.4
	100	67.5	69.6	65.4	67.8	61.4	62.5	54.7	60.3
	150	71.4	72.8	70.9	71.7	69.8	70.9	56.8	61.5
	200	74.2	76.1	73.2	75.4	70.3	72.4	58.6	62.6
	250	77.7	79.4	76.9	78.8	71.2	75.2	59.4	63.1
	300	81.3	83.1	79.0	79.4	73.9	77.8	60.8	65.8
	400	85.5	86.3	80.1	80.9	74.6	78.4	61.4	66.5
	500	87.3	90.8	80.9	84.6	76.2	79.3	62.5	67.2
III	25	61.8	63.6	60.4	60.9	53.1	55.0	48.2	52.2
	50	65.4	66.6	62.7	63.8	55.9	57.3	50.2	54.1
	100	67.8	69.0	63.9	65.8	61.3	61.2	54.1	55.7
	150	68.6	70.3	67.4	69.8	62.8	65.0	54.9	58.3
	200	70.3	72.3	68.9	70.9	63.5	66.1	57.3	59.6
	250	71.7	74.9	70.2	73.8	64.5	67.8	58.8	60.8
	300	73.1	77.9	71.8	79.6	66.4	69.4	59.7	62.3
	400	76.0	80.4	73.9	80.8	68.3	70.5	60.3	63.8
	500	81.6	83.5	80.1	81.4	69.3	72.6	61.0	64.9

All the three compounds inhibited the corrosion of mild steel in 1 M hydrochloric acid at all concentrations. It has been observed that the IE for **I**, **II**, and **III** increased with an increase in inhibitor concentration. Maximum IE for each compound was observed at 500 ppm, and any further increase in concentration did not cause any appreciable change in the performance of the inhibitor thereby indicating the attainment of the limiting value. This may be due to the formation of monolayer film over the entire mild steel surface at this concentration (Ref 8).

The IE followed the order of **I** > **II** > **III**. The decrease of IE with increase of temperature weakens physical adsorption process as evident from Table 1 and Fig. 3 suggesting a physisorption mechanism (Ref 3, 9).

All the tested compounds contain two phenyl rings—oxime nitrogen, oxime oxygen—and ring nitrogen. It is apparent from the molecular structure of these compounds that the corrosion inhibition is due to the presence of N, O, and aromatic rings. The presence of a free electron pair on the nitrogen atom, oxygen atom, and the π-electrons of phenyl ring favors the adsorption of the inhibitor, which results in the formation of a stable film (insoluble layer) on the metal surface (Ref 10, 11), favoring chemisorption. Moreover, the experimental results are in good agreement with the Temkin's adsorption isotherm. The slope of the isotherm deviates from unity. This deviation may be explained on the basis of interaction between the adsorbed species on the metal surface by mutual repulsion or attraction. Hence, from the arguments, it is clear that there is a competition between physical and chemical adsorption processes. To conclude the same, the free energy of adsorption (ΔG_{ads}) was calculated using the same isotherm. The negative value of ΔG_{ads} (around 35 kJ/mol as mentioned in Table 2) indicated the spontaneous adsorption of inhibitor on the surface of mild steel (Ref 12, 13), and it is likely that both modes of adsorption are operative to inhibit corrosion process (Ref 14).

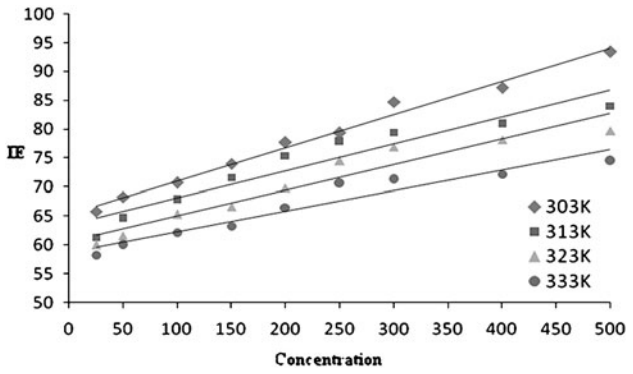

Fig. 3 A representative plot showing variations of IE of compound **I** against various temperatures for 2-h duration

3.3 Polarization Curves

Electrochemical parameters such as corrosion potential (E_{corr}), cathodic and anodic Tafel slopes (b_c and b_a), corrosion current density (i_{corr}) obtained by extrapolation of the Tafel lines, and the calculated IE are shown in Table 3. Polarization curves of the mild steel electrode in 1 M hydrochloric acid without and with addition of compounds **I**, **II**, and **III** at different concentrations are shown in Fig. 4(a)-(c), respectively. The figures depict that both cathodic and anodic reactions of mild steel corrosion are inhibited with the increase of oxime concentration in 1 M hydrochloric acid. The results suggest that the addition of piperidin-4-one derivatives reduces anodic dissolution and also retards the hydrogen evolution reaction. Tafel lines of nearly equal slopes were obtained, indicating that the hydrogen evolution reaction was activation controlled. There is no particular trend in Tafel slopes, which indicates that the inhibitor molecules are involved in simple blocking of the reaction site (Ref 15, 16). The i_{corr} values decreased considerably with increasing concentration of oximes due to adsorption (Ref 17). No definite trend was observed in the shift of E_{corr} values, in the presence of various concentrations of these inhibitors in 1 M hydrochloric acid solutions. This result indicated the mixed mode of action of these inhibitors in 1 M hydrochloric acid with the corrosion inhibiting efficiency in the following order **I** > **II** > **III**.

Thus, all the oximes with potential sites for inhibition such as oxime nitrogen, ring nitrogen, oxime oxygen, and phenyl rings behave as good corrosion inhibitors with compound **I** to be an excellent inhibitor. It is clear from Fig. 1 that compound **I** possesses less steric hindrance at C-3 of piperidine moiety as compared with **II** (having two methyl groups) and **III** (having one isopropyl group). On correlating experimental results with molecular structures it can be concluded that the increase of steric hindrance at C-3 of piperidine ring decreases corrosion inhibiting ability of the studied oximes. Further in compound **I**, electron releasing methyl group present at C-1 of piperidine moiety increases the basicity of ring nitrogen, which is also lacking in compounds **II** and **III** thus justifying the higher IE of the compound **I**.

3.4 Impedance Measurements

Nyquist plots of mild steel in uninhibited and inhibited acidic solutions containing various concentrations of **I**, **II**, and **III** are given in Fig. 5(a)-(c), respectively. From the figures, it is clear that the Nyquist plots are not perfect semicircles. According to the theory of EIS, real condenser that has charge distribution on both plates yield perfect semicircle. However, during corrosion, formation of a double layer at the metal/solution interface occurs unevenly due to dispersing effect causing imperfect semicircles (Ref 18) as seen in Fig. 5. The R_{ct} values increased as the concentrations of inhibitors

Table 2 Free energy of adsorption calculated using Temkin's adsorption isotherm

	30 °C		40 °C		50 °C		60 °C	
Inhibitor	**1 h, kJ/mol**	**2 h, kJ/mol**	**1 h, kJ/mol**	**2 h, kJ/mol**	**1 h, kJ/mol**	**2 h, kJ/mol**	**1 h, kJ/mol**	**2 h, kJ/mol**
I	27.8	28.2	29.8	29.8	32.3	31.2	33.2	34.5
II	28.2	28.6	29.8	29.6	31.9	30.5	35.9	36.4
III	32.4	31.0	32.4	30.1	33.1	32.1	35.0	36.5

Table 3 Electrochemical parameters determined for corrosion of mild steel using studied oximes

Inhibitor	Concentration	$-E_{corr}$, mV	i_{corr}, μA/cm^2	b_a, mV/dec	b_c, mV/dec	C_{dl}, μF/cm^2	R_{ct}, Ω cm^2	IE using R_{ct}
I	0	510	1995	134	198	616	17.5	…
	25	506	1258	136	200	300	25.0	30.0
	50	495	1000	172	218	238	30.5	42.6
	100	496	794	138	194	135	67.5	74.1
	150	497	631	128	180	104	87.5	80.0
	200	494	562	114	142	96	95.0	81.6
	250	496	501	116	156	70	107.5	83.7
	300	496	398	112	132	66	137.5	87.3
	400	494	355	116	134	60	152.5	88.5
	500	489	316	84	96	53	172.5	89.9
II	25	493	1413	124	144	358	31.0	43.5
	50	491	1122	64	86	274	40.5	56.8
	100	488	891	72	92	179	62.0	71.8
	150	488	794	90	90	156	71.0	75.4
	200	487	631	58	46	143	114.0	84.6
	250	488	562	36	54	127	128.0	86.3
	300	483	447	74	92	123	133.0	86.8
	400	480	398	58	60	112	145.0	87.9
	500	479	355	52	50	72	155.0	88.7
III	25	490	1778	90	110	347	31.0	43.5
	50	489	1585	78	92	264	42.0	58.3
	100	483	1413	96	118	222	50.0	65.0
	150	480	1122	136	120	216	62.0	71.8
	200	483	1000	84	96	209	64.0	72.7
	250	480	891	84	96	157	70.5	75.2
	300	484	708	52	56	137	81.0	78.4
	400	493	562	102	72	103	87.0	79.9
	500	502	501	82	80	100	92.0	81.0

increased, whereas the values of C_{dl} decreased with an increase in the inhibitors concentration in all the three oximes. This situation was a result of increasing surface coverage by the inhibitors leading to an increase in IE which is in agreement with the reports of Bothi Raja and Sethuraman (Ref 17, 19) and Senthilkumar et al. (Ref 16). A decrease in the local dielectric constant and/or an increase in the thickness of the electrical double layer can cause this decrease in the C_{dl}, suggesting that compounds **I**, **II**, and **III** function by adsorption at the metal/solution interface (Ref 20, 21). The decrease in C_{dl} values was caused by the gradual replacement of water molecules by the adsorption of the organic molecules on the metal surface, decreasing the extent of dissolution reaction (Ref 5, 22). The adsorption of oxime molecules at a metal solution interface can be represented as a substitutional adsorption process between the oxime molecules in the aqueous solution ($OX_{(sol)}$) and the water molecules on the metallic surface ($H_2O_{(ads)}$).

$$OX_{(sol)} + nH_2O_{(ads)} \leftrightarrow OX_{(ads)} + nH_2O_{(sol)} \quad \text{(Eq 2)}$$

where $OX_{(sol)}$ and $OX_{(ads)}$ are the oxime molecules in the aqueous solution and those adsorbed on the metallic surface, respectively. $H_2O_{(ads)}$ is the water molecules on the metallic surface, and n is the size ratio representing the number of water molecules replaced by one molecule of oxime adsorbate. Hence, the studied molecules can adsorb on the metal surface in two different ways. First, the inhibitor molecules can compete with chloride ions for sites at the water covered anodic surface. In doing so, the protonated inhibitor loses its associated proton in entering the double layer and can adsorb chemically by donating electrons to the metal. Second, the protonated inhibitor electrostatically can also adsorb onto the negatively charged mild steel surface, through its cationic form (Ref 23).

Moreover, Fig. 5(c) shows an imperfect semicircle due to the presence of inductive loop at low frequency region. This is attributed to adsorption-desorption process at the surface of the electrode which leads to electrode/electrolyte interface modification (Ref 24). The positive value of Z imaginary axis indicates that the double layer capacitance and charge transfer resistance are held in parallel as depicted in Fig. 2.

3.5 XRD Analysis

XRD pattern for polished mild steel specimen, shown in Fig. 6(a), revealed the characteristic 2θ values for Fe (44.9°, 65.1°, and 82.6°). The absence of these peaks in Fig. 6(b) for mild steel specimen exposed to inhibitor solution clearly depicts the formation of protecting film by the oxime-supporting chemisorption mechanism in addition to physical adsorption. The non-appearance of the characteristic peak of Fe in Fig. 6(b) may be due to the amorphous nature of Fe-oxime complex (Ref 25).

3.6 SEM with EDS

Micrograph shown in Fig. 7(a) depicts the surface morphology of mild steel specimen under brightly polished condition. Field view of above picture shows the mechanical polishing nicks before immersion. EDS detected mainly the iron substrate without oxidation in all the selected areas. Figure 7(b) shows the extent of damage of mild steel surface caused by 1 M hydrochloric acid. The EDS analysis for

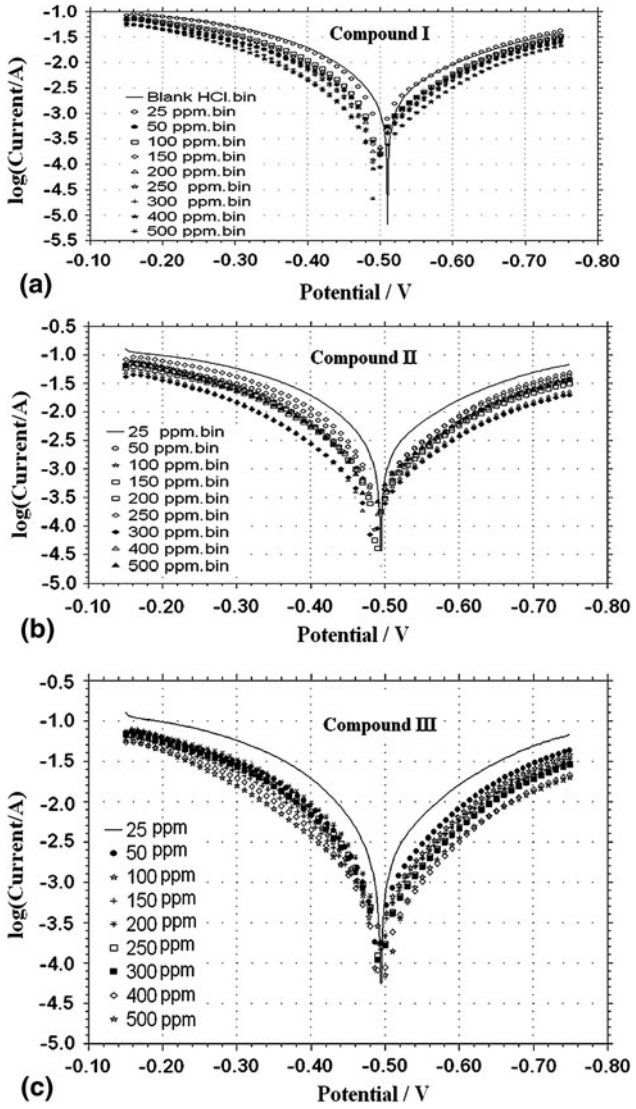

Fig. 4 Tafel lines for mild steel corrosion in 1 M hydrochloric acid in the absence and the presence of various concentration of inhibitor

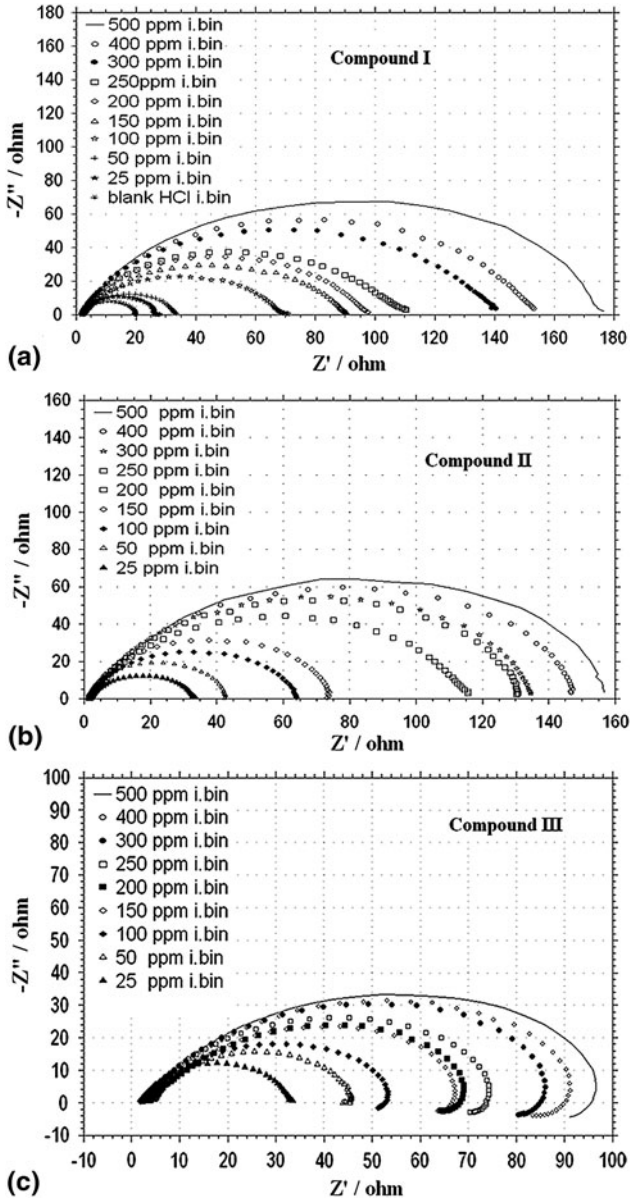

Fig. 5 Nyquist plots for mild steel corrosion in 1 M hydrochloric acid in the absence and the presence of various concentration of inhibitor

elements in the selected areas, viz., spot 1, spot 2, and spot 3 (Table 4), revealed the presence of Fe in its oxidized form due to rusting. The selected areas of Fig. 7(b) contain Cl besides Fe. This indicates the formation of hydrated corrosion products of Fe and Cl. Surface morphology of mild steel specimen exposed to 500 ppm of compound **I** in acid solution is depicted in Fig. 7(c). EDS analysis of the same in the selected area (spot 1) contains Fe under slightly oxidized state as evident from Table 4. The selected areas viz., spot 2 and spot 3, still possess Fe phases in oxidized condition. However, all the selected areas in Fig. 7(c) have lesser Cl content as compared to blank. This reveals the formation of protective layer by compound **I** on the mild steel surface.

3.7 Quantum Chemical Calculation

Higher HOMO energy (E_{HOMO}) of the inhibitor indicates the higher electron donating ability (Ref 26, 27). Considering the electron-donating abilities of the compounds **I**, **II**, and **III**, E_{HOMO} is an important parameter in influencing inhibition efficiencies. Inhibitor **I**, having the highest HOMO energy,

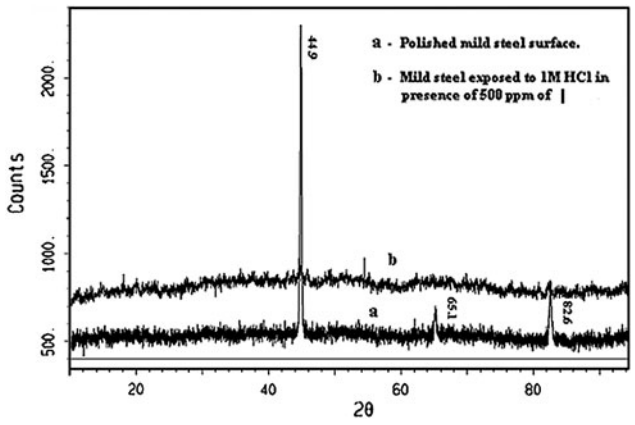

Fig. 6 XRD pattern for mild steel specimen in polished condition and exposed to corrosive medium in the presence of inhibitor

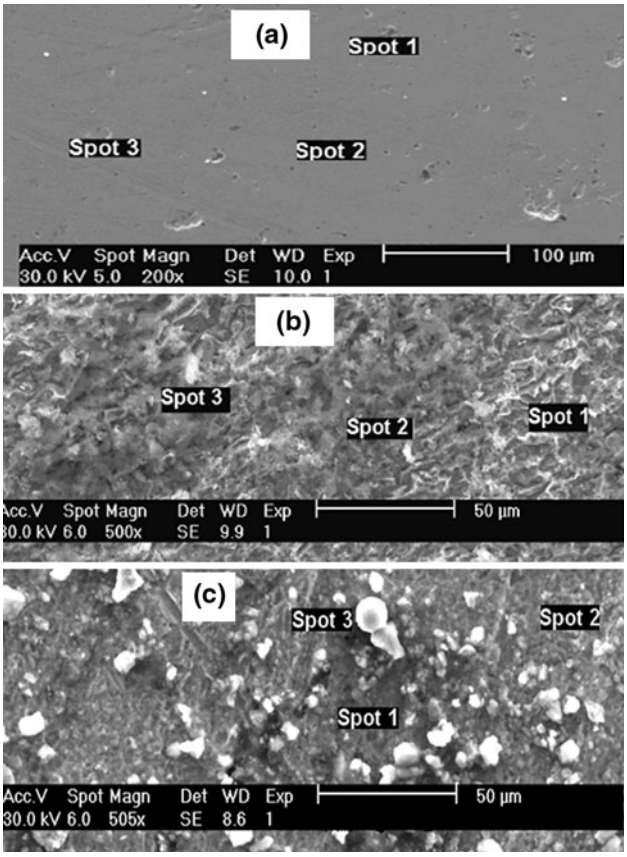

Fig. 7 SEM micrographs of mild steel specimens under (a) brightly polished condition, (b) blank hydrochloric acid, and (c) 500 ppm of inhibitor **I**

Table 4 EDS results corresponding to Fig. 5 (wt.% normalized)

Description	Figure No.	Selected area	Fe	Cl	Si	Mn
Polished specimen	7(a)	Spot 1	99.24	…	0.36	0.40
		Spot 2	99.12	…	0.39	0.49
		Spot 3	98.73	…	0.63	0.64
Specimen with blank acid	7(b)	Spot 1	90.52	9.48	…	…
		Spot 2	92.18	7.82	…	…
		Spot 3	93.44	6.56	…	…
Specimen with compound **I**	7(c)	Spot 1	95.64	4.36	…	…
		Spot 2	96.32	3.68	…	…
		Spot 3	96.06	3.94	…	…

donates electrons easily, and inhibits corrosion process effectively compared to the other two oximes. The results obtained from quantum chemical calculations are listed in Table 5. The energy gap between LUMO and HOMO ($\Delta E = E_{LUMO} - E_{HOMO}$) of the inhibitor also plays a role in deciding the IE. The smaller ΔE values could cause higher IE (Ref 28). However, correlation of HOMO and LUMO with IE of the studied oximes is not the only way to study the performance of inhibitor. Certain in situ conditions have also to be considered. In this study also, there may be a competition for adsorption sites on mild steel surface between anions of acids and oximes. Iron can act as a Lewis base while the oximes can act as Lewis

Table 5 Electron density values calculated using AM1 method

Compound	E_{HOMO}, eV	E_{LUMO}, eV	ΔE, eV	Fe_{HOMO}-$Oxime_{LUMO}$, eV
I	−9.139670	0.343447	9.483117	−8.15345
II	−9.193105	0.277607	9.470712	−8.08761
III	−9.323388	0.353270	9.676658	−8.16327

E_{HOMO} of Fe is −7.81 eV (Ref 33)

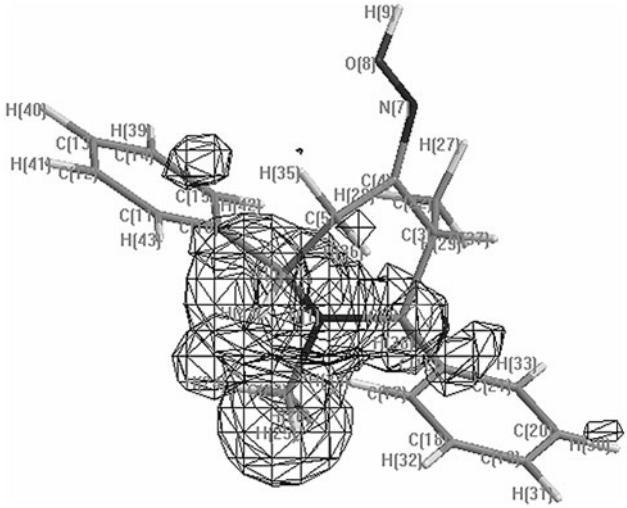

Fig. 8 Electron distribution in compound **I** obtained AM1 semi empirical method

acids. Therefore, the donor and acceptor interactions in the presence of other ions can be interpreted using E_{HOMO} and E_{LUMO} of iron and oximes for deciding about the nature of inhibition. Stronger covalent bonding can be expected only if the absolute value of Fe_{HOMO}-$Oxime_{LUMO}$ gap is approximately 0 eV (Ref 29, 30). However, from Table 5, it is clear that the difference of Fe_{HOMO}-$Oxime_{LUMO}$ gap is in the range of 8 eV which shows that there is probably a certain percentage of ionic character. It has been reported that the adsorption of chloride ions on iron increases its softness (Ref 31). This is due to the electrostatic adsorption between chlorides present in the medium and protonated oxime molecules as stated earlier. Hard and soft acids and bases (HSAB) principle states that the soft molecules have the HOMO orbital relatively higher in energy (Ref 32). This means that the HOMO-LUMO gap of the iron should decrease upon electrostatic adsorption of chlorides. Hence, the absolute value of the Fe_{HOMO}-$Oxime_{LUMO}$ gap will reduce, and consequently, the attraction between the iron surface covered by chloride ions and the protonated oximes will have an increasing percentage of covalent character.

HOMO electron distribution of compound **I** is shown in Fig. 8 (wire mesh area), which revealed that ring nitrogen and phenyl rings can act as probable centers for electron donation thus aiding inhibition.

3.8 Analysis of FT-IR Spectra

The compound **I** displayed (Fig. 9) the characteristic absorption IR band for C=N bond, aromatic C-H stretching, and −N-OH stretching around 1673 cm^{-1}, appearing at

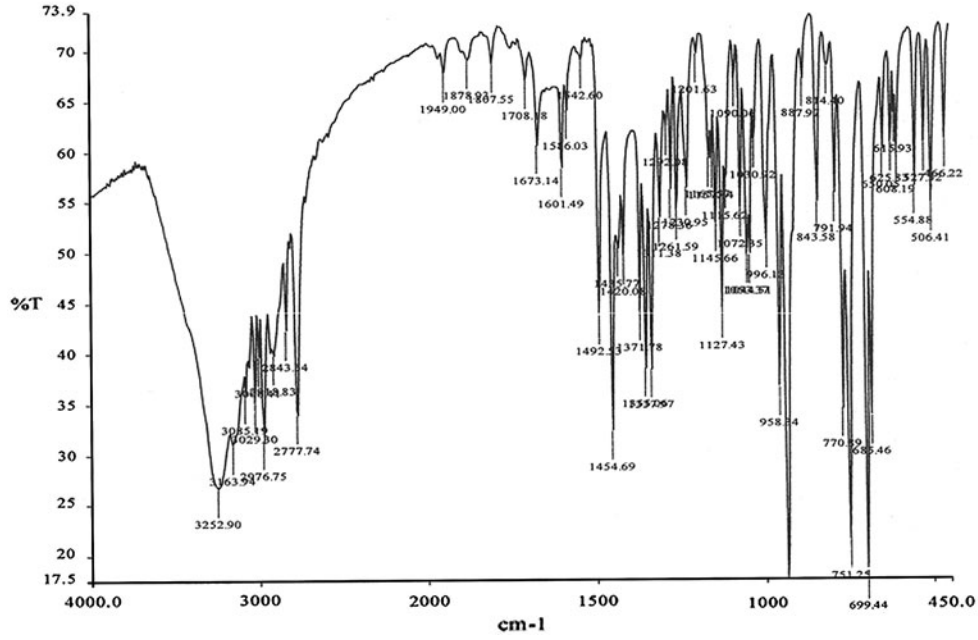

Fig. 9 IR spectra of compound **I**

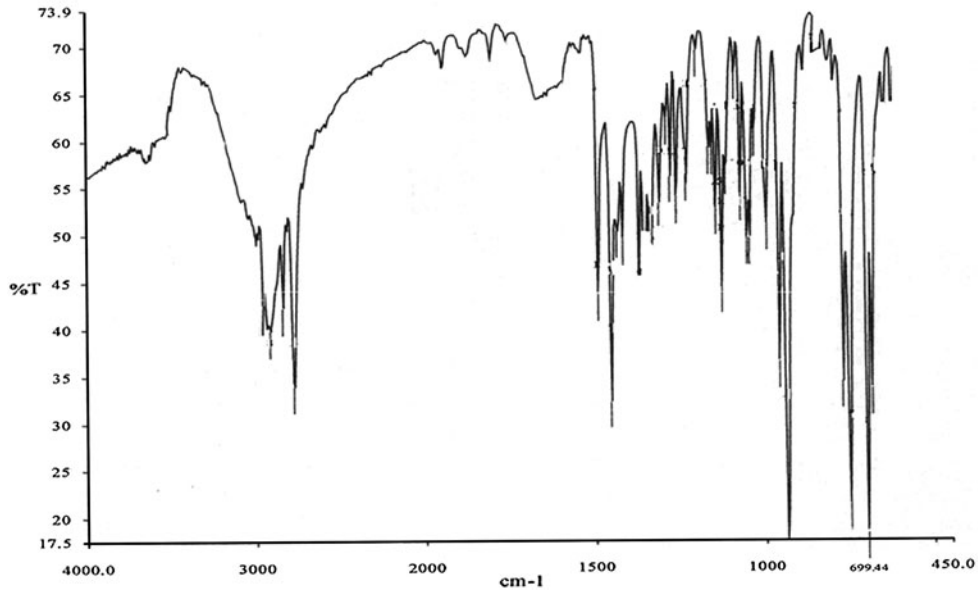

Fig. 10 IR spectra of film formed by compound **I** on the mild steel surface

3085 cm^{-1}, and 3252 cm^{-1} respectively. The absence of bands (Fig. 10) at 1673 and 3252 cm^{-1} suggest that the lone pair of electrons present in the nitrogen is utilized for the bond formation with Fe atoms present in mild steel supporting the protective film formation through chemisorption.

4. Conclusion

From the results, it is clear that all the studied oximes serve as effective corrosion inhibitors in 1 M hydrochloric acid medium with compound **I** having higher IE when compared with the other two. Potentiodynamic polarization curves indicated the mixed mode of inhibition by all the oximes. Nyquist plots supported the inhibition of corrosion through adsorption by the decrease of C_{dl} values with increase of inhibitor concentration. Thermodynamic parameters indicated that both physisorption and chemisorption modes are operative to inhibit corrosion process. FT-IR, XRD, and SEM with EDS gave the supportive evidence for the formation of protective film. Quantum chemical study revealed that ring nitrogen and phenyl rings were the potential sites to control the corrosion process.

Acknowledgments

The authors thank the authorities of Gandhigram Rural University for their help and encouragement. The authors acknowledge the help received from Dr. Vijayalakshmi, Dr. Parameswaran, and Ms. Radhika, PMD Division, IGCAR, Kalpakkam and for the permission to use the instrumental facilities. Authors (ANS and KT) thank the authorities of SASTRA University, Thanjavur for the support.

References

1. P. Bothi Raja and M.G. Sethuraman, Atropine Sulphate as Corrosion Inhibitor for Mild Steel in Sulphuric Acid Medium, *Mater. Lett.*, 2008, **62**(10–11), p 1602–1604
2. P. Bothi Raja and M.G. Sethuraman, Inhibitive Effect of Black Pepper Extract on the Sulphuric Acid Corrosion of Mild Steel, *Mater. Lett.*, 2008, **62**(17–18), p 2977–2979
3. A.N. Senthilkumar and M.G. Sethuraman, Corrosion Inhibition Potential of Sulfadimidine, *Corros. Rev.*, 2008, **26**(1), p 23–37
4. N. Hackerman and R.M. Hurd, *Proceedings of International Congress on Metallic Corrosion*, Butterworth, London, 1962, p 166
5. S. Muralidharan, K.L.N. Phani, S. Pitchumani, S. Ravichandran, and S.V.K. Iyer, Polyamino-Benzoquinone Polymers: A New Class of Corrosion Inhibitors, *J. Electrochem. Soc.*, 1995, **142**(5), p 1478–1483
6. J. Jayabharathi, A. Manimekalai, T. Consalata Vani, and M. Padmavathy, Synthesis, Stereochemistry and Antimicrobial Evaluation of t(3)-Benzyl-r(2), c(6)-Diaryl-piperidin-4-one and Its Derivatives, *Eur. J. Med. Chem.*, 2007, **42**(5), p 593–605
7. V. Baliah and C.R. Noller, The Preparation of Some Piperidine Derivatives by the Mannich Reaction, *J. Am. Chem. Soc.*, 1948, **70**(11), p 3853–3855
8. A.K. Maayta and N.A.F. Rawashdeh, Inhibition of Acidic Corrosion of Pure Aluminium by Some Organic Compounds, *Corros. Sci.*, 2004, **46**, p 1129–1140
9. E.E. Ebenso, P.C. Okafer, and U.F. Ekpe, Studies on the Inhibition of Aluminium Corrosion by 2-Acetylpheno Thiazine in Chloro Acetic Acid, *Anti-Corros. Meth. Mater.*, 2003, **50**(6), p 414–421
10. S. Muralidharan, M.A. Quraishi, and S.V.K. Iyer, The Effect of Molecular Structure on Hydrogen Permeation and the Corrosion Inhibition of Mild Steel in Acidic Solutions, *Corros. Sci.*, 1995, **37**(11), p 1739–1750
11. S. Rengamani, S. Muralidharan, M. Anbukulandainathan, and S.V.K. Iyer, Inhibiting and Accelerating Effects of Amino Phenols on the Corrosion and Permeation of Hydrogen Through Mild Steel in Acidic Solutions, *J. Appl. Electrochem.*, 1994, **24**(4), p 355–360
12. M. Elachouri, M.S. Hajji, M. Salem, S. Kertit, J. Aride, R. Coudert, and E. Essassi, Some Nonionic Surfactants as Inhibitors on the Corrosion of Iron in Acid Chloride Solutions, *Corrosion*, 1996, **52**(2), p 103–108
13. B.V. Savithri and S. Mayanna, Tetra Butyl Ammonium Iodide Cetyl Pyridinium Bromide and Cetyl Tri Methyl Ammonium Bromide as Corrosion Inhibitors for Mild Steel in Sulphuric Acid Medium, *Ind. J. Chem. Technol.*, 1996, **3**(5), p 256–258
14. S.Z. Duan and Y.L.Tao, *Interface Chemistry*, Higher Education Press, Beijing, 1990, p 124–126
15. F.M. Bayoumi and W.A. Ghanem, Corrosion Inhibition of Mild Steel Using Naphthalene Disulfonic Acid, *Mater. Lett.*, 2005, **59**(29–30), p 3806–3809
16. A.N. Senthilkumar, K. Tharini, and M.G. Sethuraman, Corrosion Inhibitory Effect of Few Piperidin-4-one Oximes on Mild Steel in Hydrochloric Acid Medium, *Surf. Rev. Lett.*, 2009, **16**(1), p 141–147
17. P. Bothi Raja and M.G. Sethuraman, Inhibition of Corrosion of Mild Steel in Sulphuric Acid Medium by *Calotropis procera*, *Pig. Res. Technol.*, 2009, **38**(1), p 33–37
18. P. Bothi Raja and M.G. Sethuraman, Corrosion Inhibition of Mild Steel by *Datura metel* (Leaves) in Acidic Medium, *Pig. Res. Technol.*, 2005, **34**(6), p 327–331
19. P. Bothi Raja and M.G. Sethuraman, Studies on the Inhibitive Effect of *Datura stramonium* Extract on the Acid Corrosion of Mild Steel, *Surf. Rev. Lett.*, 2007, **14**(6), p 1157–1164
20. H. Ashassi-Sorkhabi, B. Shaabani, and D. Seifzadeh, Effect of Some Pyrimidinic Shciff Bases on the Corrosion of Mild Steel in Hydrochloric Acid Solution, *Electrochim. Acta*, 2005, **50**(16–17), p 3446–3452
21. E. McCafferty and N. Hackerman, Double Layer Capacitance of Iron and Corrosion Inhibition with Polymethylene Diamines, *J. Electrochem. Soc.*, 1972, **119**, p 146–154
22. M. Lagrenee, B. Mernari, M. Bouanis, M. Traisnel, and F. Bentiss, Study of the Mechanism and Inhibiting efficiency of 3,5-Bis(4-methyl thiophenyl)-4H-1,2,4-triazole on Mild Steel Corrosion in Acid Media, *Corros. Sci.*, 2002, **44**(3), p 573–588
23. M. Ozcan and I. Dehri, Electrochemical and Quantumchemical Studies on Some Sulphur Containing Organic Compounds as Inhibitors for the Acid Corrosion of Mild Steel, *Prog. Org. Coat.*, 2004, **51**(3), p 181–187
24. A. Lgamri, H. Abou El Makarim, A. Guenbour, A. Ben Bachir, L. Aries, and S. El Hajjaji, Electrochemical Study of the Corrosion Behaviour of Iron in Presence of New Inhibitor in 1 M HCl, *Prog. Org. Coat.*, 2003, **48**, p 63–70
25. A.A. Rahim, E. Rocca, J. Steinmetz, M.J. Kassim, R. Adnan, and M. Sani Ibrahim, Mangrove Tannins and Their Flavanoid Monomers as Alternative Steel Corrosion Inhibitors in Acidic Medium, *Corros. Sci.*, 2007, **49**(2), p 402–417
26. N. Khalil, Quantum Chemical Approach of Corrosion Inhibition, *Electrochim. Acta*, 2003, **48**(18), p 2635–2640
27. J. Vosta and N. Hackerman, The Dependence of Capacitance on Time in an Acid Inhibition Corrosion Process, *Corros. Sci.*, 1990, **30**(8–9), p 949–950
28. J. Fang and L. Jie, Quantum chemistry Study on the Relationship Between Molecular Structure and Corrosion Inhibition of Amides, *J. Mol. Struct.*, 2002, **593**(1–3), p 179–185
29. G. Klopman, Chemical Reactivity and the Concept of Charge and Frontier Controlled Reactions, *J. Am. Chem. Soc.*, 1968, **90**(2), p 223–234
30. W.B. Jensen, The Lewis Acid-Base Definitions: A Status, *Chem. Rev.*, 1978, **78**(1), p 1–22
31. K. Aramaki, T. Mochizuki, and H. Nishihara, Impedance Study on Inhibition and Stimulation of Iron Corrosion in Acid Solution by Various Inorganic Anions and Tetra-alkyl ammonium Cation, *J. Electrochem. Soc.*, 1988, **135**(6), p 1364–1369
32. R.G. Pearson, Recent Advances in the Concept of Hard and Soft Acids and Bases, *J. Chem. Educ.*, 1987, **64**(7), p 561–567
33. P. Mutombo and N. Hackerman, The Effect of Some Organo Phosphorous Compounds on the Corrosion Behaviour of Iron in 6 M HCl, *Anti-Corros. Meth. Mater.*, 1998, **45**(6), p 413–418